

**NASA  
Technical  
Paper  
3210**

1992

# Stiffness and Strength Tailoring in Uniform Space-Filling Truss Structures

Mark S. Lake  
*Langley Research Center  
Hampton, Virginia*

**NASA**

National Aeronautics and  
Space Administration  
Office of Management  
Scientific and Technical  
Information Program



## Summary

This paper presents a deterministic procedure for tailoring the continuum stiffness and strength of uniform space-filling truss structures through the appropriate selection of truss geometry and member sizes (i.e., flexural and axial stiffnesses and length). The trusses considered herein are generated by uniform replication of a characteristic truss cell. The repeating cells are categorized by one of a set of possible geometric symmetry groups derived using crystallographic techniques. The elastic symmetry associated with each geometric symmetry group is identified to help select an appropriate truss geometry for a given application. Stiffness and strength tailoring of a given truss geometry is enabled through explicit expressions relating the continuum stiffnesses and failure stresses of the truss to the stiffnesses and failure loads of its members. These expressions are derived using an existing equivalent continuum analysis technique and a newly developed analytical failure theory for trusses. Several examples are presented to illustrate the application of these techniques and to demonstrate the usefulness of the information gained from this analysis.

## Introduction

In the future, the primary structures of many large orbiting spacecraft will be lightweight trusses. Although numerous studies have been performed to determine the feasibility and structural characteristics of these trusses (e.g., refs. 1 through 3), little work has been done to establish deterministic procedures for their design. The selection of appropriate truss designs is influenced by both structural optimization and spacecraft operational considerations. Currently, structural optimization of these trusses is a predominantly heuristic process involving trial and error procedures. This paper presents a deterministic procedure for truss geometry selection and member design based on tailoring the continuum stiffness and strength characteristics of the truss. Analysis of the truss stiffness and strength characteristics is performed using an equivalent continuum analogy (ref. 4). This approach is preferred because it offers better insight into structural behavior than the conventional numerical analysis techniques offer.

The trusses considered herein are generated by uniform rotational and/or translational replication of a characteristic cell, as shown in figure 1, and they are thus called uniform space-filling trusses. In most cases, the repeating truss cell and the resulting truss structure inherently possess some geometric symmetry. The presence of geometric symmetry implies elastic symmetry that reduces the number of independent equivalent elastic constants characterizing the truss. In this study, the crystallographic techniques are used to define the possible geometric symmetry groups associated with repeating cells that generate uniform trusses. In addition, the number of independent elastic constants associated with each geometric symmetry group is identified to help select an appropriate truss geometry for a given application.

The independent elastic constants characterizing a truss can be tailored to specific values by selecting appropriate member stiffnesses. In the present study, this stiffness tailoring is accomplished using explicit relationships between the equivalent continuum stiffnesses of a truss and the axial stiffnesses of its members. Also, the continuum strength characteristics of a truss are tailored using a strength tensor that is written explicitly in terms of the local elastic buckling loads of the truss members. To illustrate the application of these techniques, a commonly used truss geometry is analyzed to determine member sizes that produce optimum isotropic and orthotropic (i.e., one direction of high stiffness and strength) designs.

All derivations presented have been performed symbolically using a computerized mathematics routine (ref. 5), and results have been converted into a numerical form when necessary. The advantage in using symbolic algebra is that explicit relationships can be determined between the design parameters and the continuum elastic behavior of the truss. These explicit relationships significantly enhance the utility of the stiffness and strength tailoring procedures presented.

## Symbols

$A$	cross-sectional area of members in regular octahedral truss
$A_c$	cross-sectional area of members in cubic lattice of Warren truss
$A_n$	cross-sectional area of members in $n$ th group
$A_o$	cross-sectional area of members in octahedral lattice of Warren truss
$C_{ijkl}$	continuum elastic stiffnesses (tensor form)
$C'_{ijkl}$	transformed continuum elastic stiffnesses
$(C'_{1111})_n$	continuum unidirectional stiffness for $n$ th group of parallel members
$c_{mn}$	continuum elastic stiffnesses (matrix form)
$E$	Young's modulus of truss material
$E_{eq}$	equivalent continuum Young's modulus
$(E_{eq})_{iso}$	equivalent Young's modulus of isotropic Warren truss
$(E_{eq})_z$	equivalent $z$ -direction Young's modulus
$G_{eq}$	equivalent continuum shear modulus
$L$	characteristic dimension of truss repeating cell
$l_n$	length of members in $n$ th group
$r_n$	radius of gyration of members in $n$ th group
$S_{ijkl}$	continuum elastic compliances (tensor form)
$s_{mn}$	continuum elastic compliances (matrix form)
$T_{ij}$	coordinate transformation tensor
$v_n$	volume fraction of $n$ th group of parallel members
$x, y, z$	Cartesian coordinates
$x'$	member longitudinal direction
$\beta$	length ratio of repeating truss cell in $z$ direction
$\delta_c$	ratio of cross-sectional areas of members in Warren truss
$\delta_n$	ratio of cross-sectional areas of members in $n$ th group to that of first group
$\varepsilon_{ij}$	strain tensor
$\varepsilon'_{ij}$	transformed strain tensor
$(\varepsilon_{crit})_n$	critical axial strain for $n$ th group of members
$\nu_{eq}$	equivalent continuum Poisson's ratio
$\rho$	density of truss material
$\rho_{eq}$	equivalent continuum density
$\sigma_{ij}$	stress tensor
$\sigma_{ult}$	continuum compression strength

$(\sigma_{\text{ult}})_z$	$z$ -direction compression strength
$(\sigma_{\text{ult}})_{\text{iso}}$	compression strength of isotropic Warren truss
$\phi_i$	direction cosine with the $i$ th coordinate axis
$\theta, \varphi$	spherical coordinates
$[\Omega_{kl}]_n$	strength tensor

## Truss Geometry Selection

The design of a truss is often governed by considerations other than the structural performance (e.g., as shown in ref. 6). For example, operational concerns such as the arrangement and integration of spacecraft subsystems onto a truss might dictate a particular geometry for the truss repeating cell. For applications in which operational concerns do not dominate, selecting a truss geometry by matching its inherent elastic behavior with the structural requirements of the spacecraft is prudent. Even in situations in which operational concerns prevail, enough latitude probably exists in the selection of a truss geometry so that structural considerations can be incorporated. This section categorizes the elastic characteristics of most uniform space-filling truss structures by examining their geometric symmetry.

The uniform truss structures considered herein are similar to crystalline lattices because they both can be generated by replicating a characteristic repeating cell that typically possesses geometric symmetry. Of interest are symmetry with respect to specific rotations about one or more axes and symmetry with respect to reflection about one or more planes. Symmetry in the truss geometry (i.e., lattice arrangement and member designs) implies symmetry in the elastic characteristics of the truss. This implied elastic symmetry reduces the number of independent equivalent elastic constants characterizing the continuum behavior of the truss, and it thus simplifies the task of stiffness and strength tailoring.

### Rotational Symmetry Groups

Crystallographic studies (refs. 7 and 8) have shown that the rotational and reflectional symmetries in reticulated, or discrete, structures are limited to a set of 32 possible combinations that are commonly called crystallographic symmetry groups. Love (ref. 9) determined that the elastic behavior of most crystallographic symmetry groups can be derived by considering only rotational symmetry. For brevity, the few cases in which reflectional symmetry is important are not considered herein. By neglecting reflectional symmetry, the 32 crystallographic symmetry groups reduce to the 10 rotational symmetry groups shown in figure 2.

Each symmetry group in figure 2 is identified by a specific combination of axes about which rotational symmetry exists. The orientations of these axes are shown relative to a Cartesian coordinate system, and the order of rotational symmetry is given by one of four graphical symbols: a cusped oval, a triangle, a square, or a hexagon. These symmetry symbols are related to the order of symmetry in the key. This order of symmetry is defined as  $n$ -gonal where the rotation angle is  $2\pi/n$  and  $n$  is either 2, 3, 4, or 6. Notice that in symmetry groups  $i$  and  $j$ , the trigonal symmetry axes lie along lines connecting the center of a cube with its corners, thus structures of these symmetry groups are often referred to as cubic structures.

Symmetry groups that possess more than one axis of rotational symmetry are called multi-axial. The three rotational symmetry axes presented for each of the multi-axial groups are not the only symmetry axes for those groups. A complete set can be generated by applying the symmetry operation of each axis to the others. For example, in symmetry group  $d$ , applying trigonal symmetry about the  $z$ -axis identifies four additional digonal symmetry axes separated by  $60^\circ$  in the  $x$ - $y$  plane.

Any truss structure that possesses axes of rotational symmetry can be categorized by one of the 10 rotational symmetry groups in figure 2. This classification is accomplished by identifying all rotational symmetry axes within the structure and then by selecting a Cartesian coordinate system relative to these axes which matches one of the given symmetry groups. Once the symmetry group of the truss is identified, its inherent elastic behavior is determined using the methods that follow.

### Elastic Characteristics of Rotational Symmetry Groups

A uniform truss structure can be represented by an equivalent homogeneous anisotropic continuum characterized by 21 empirical elastic constants. These elastic constants appear as stiffnesses  $c_{mn}$  or  $C_{ijkl}$  in the constitutive equations given in equation (1a) in matrix form and equation (1b) in tensor form:

$$\begin{Bmatrix} \sigma_{11} \\ \sigma_{22} \\ \sigma_{33} \\ \sigma_{23} \\ \sigma_{13} \\ \sigma_{12} \end{Bmatrix} = \begin{bmatrix} c_{11} & c_{12} & c_{13} & c_{14} & c_{15} & c_{16} \\ c_{12} & c_{22} & c_{23} & c_{24} & c_{25} & c_{26} \\ c_{13} & c_{23} & c_{33} & c_{34} & c_{35} & c_{36} \\ c_{14} & c_{24} & c_{34} & c_{44} & c_{45} & c_{46} \\ c_{15} & c_{25} & c_{35} & c_{45} & c_{55} & c_{56} \\ c_{16} & c_{26} & c_{36} & c_{46} & c_{56} & c_{66} \end{bmatrix} \begin{Bmatrix} \varepsilon_{11} \\ \varepsilon_{22} \\ \varepsilon_{33} \\ 2\varepsilon_{23} \\ 2\varepsilon_{13} \\ 2\varepsilon_{12} \end{Bmatrix} \quad (1a)$$

$$\sigma_{ij} = C_{ijkl} \varepsilon_{kl} \quad (1b)$$

When the truss possesses geometric symmetry, elastic symmetry is implied, which reduces the number of independent continuum elastic constants.

A continuum that possesses geometric symmetry with respect to a rotational or a reflective transformation (characterized by  $T_{ij}$ ) also possesses symmetry in its elastic constants (see, for example, ref. 10). Therefore, the transformed stiffness tensor  $C'_{ijkl}$  must be identical to the original tensor  $C_{ijkl}$ . Hence,

$$C'_{ijkl} = C_{mnop} T_{in} T_{jn} T_{ko} T_{lp} = C_{ijkl} \quad (2)$$

The number of independent elastic constants associated with each symmetry group, presented in figure 2, is determined using equation (2). A transformation tensor  $T_{ij}$  is determined for the specified rotation about each symmetry axis and substituted into equation (2) to give 21 conditions on the stiffnesses  $C_{ijkl}$ . Some of these conditions are identically satisfied, whereas others can be satisfied only by the elimination or restriction of certain elastic constants. This process is repeated for all rotational symmetry axes in the given symmetry group, and the resulting reduced set of elastic constants defines the continuum elastic characteristics of any truss structure that is a member of that symmetry group.

For example, the independent elastic constants characterizing trusses of symmetry group *a* are determined by enforcing elastic symmetry with respect to a rotation of  $180^\circ$  about the *z*-axis. The transformation matrix for this rotation is

$$T_{ij} = \begin{bmatrix} -1 & 0 & 0 \\ 0 & -1 & 0 \\ 0 & 0 & 1 \end{bmatrix} \quad (3)$$

Substituting equation (3) into equation (2) gives the following result:

$$C_{ijkl} = C_{ijkl} \quad (4a)$$

if an even number (or none) of the indices is 3 and

$$C_{ijkl} = -C_{ijkl} \quad (4b)$$

if an odd number of the indices is 3. Satisfying equation (4b) requires the following to be true (note that, because of symmetry in  $C_{ijkl}$ , many possible permutations of the subscripts have been omitted):

$$C_{1123} = C_{1113} = C_{2223} = C_{2113} = C_{3323} = C_{3313} = C_{2312} = C_{1312} = 0 \quad (5)$$

Employing the usual conversion from tensor to matrix form (ref. 10), the following equivalent conditions exist for the components of the stiffness matrix:

$$c_{14} = c_{15} = c_{24} = c_{25} = c_{34} = c_{35} = c_{46} = c_{56} = 0 \quad (6)$$

Similar calculations can be made for the remaining symmetry groups in figure 2. Without presenting the details, the conditions on continuum stiffnesses as well as the number of independent elastic constants for each symmetry group are presented in table I. A similar derivation shows that the conditions presented in table I must also be obeyed by the components of the continuum compliance tensor.

An obvious conclusion from table I is that the presence of any symmetry in a truss lattice significantly reduces the number of independent elastic constants characterizing its continuum behavior. This result greatly simplifies the task of tailoring the stiffness and strength of most trusses. Remember that the conditions on the elastic constants presented in table I are valid only for the coordinate axes presented in figure 2. For example, symmetry groups  $b, f, g, h, i,$  and  $j$  are indicated to have zero shear coupling stiffnesses (e.g.,  $c_{14}, c_{15},$  and  $c_{16}$ ) in the given coordinate system, but they might have nonzero coupling stiffnesses in an alternate coordinate system. As explained by Rosen and Shu (ref. 11), and seen in table I, none of the permissible geometric symmetry groups possesses sufficient symmetry to ensure isotropic elastic behavior. However, this research shows that isotropy can be obtained by tailoring the relative stiffnesses of different truss members.

The information in table I should help select appropriate truss geometries for particular truss applications and determine additional stiffness tailoring requirements for the selected truss geometry. For example, if the primary loads in a truss are expected to occur in only one direction, considering geometries that have less symmetry and which can easily be tailored to have significantly higher stiffnesses and strengths in that direction (i.e., an orthotropic design) is more efficient. However, for a structure that may have to sustain loads in multiple directions or one for which the loading conditions are not well-defined, considering truss geometries that possess more symmetry and which can be tailored to behave isotropically may be best.

## Stiffness and Strength Tailoring

Once a truss geometry has been selected, its independent elastic constants are identified using table I. The values of these constants can be adjusted for a particular application by tailoring the relative axial stiffnesses of the members comprising the truss. Likewise, changing the relative elastic buckling loads of different members alters the equivalent continuum strengths of the truss. Changing only the dimensions and member stiffnesses of a truss which do not violate its geometric

symmetry causes it to remain in the same rotational symmetry group; thus, the conditions on its continuum stiffnesses given in table I remain valid. Alternatively, changing dimensions and member stiffnesses of a truss which violate its geometric symmetry changes its rotational symmetry group, thus altering the number of independent elastic constants characterizing its behavior. Stiffness and strength tailoring will be demonstrated for a truss in which geometric symmetry is maintained and one in which geometric symmetry is altered.

### Equivalent Continuum Elastic Constants

Once a candidate truss for stiffness tailoring is selected, its continuum stiffnesses are calculated in terms of the axial stiffnesses of its members. The approach used in this study for calculating these stiffnesses was developed by Nayfeh and Hefzy (ref. 12); this approach is similar to a three-dimensional generalization of classical laminated plate theory (ref. 13) in which groups of parallel members within the truss are analogous to individual lamina. Because truss members carry only axial loads, each group of parallel members forms a unidirectional elastic continuum that has no transverse or shearing stiffnesses. The truss assemblage stiffnesses are obtained by summing the stiffnesses of each of the groups of parallel members. This superposition of stiffnesses implies that the continuum displacement field within a truss is single-valued, which is consistent with the fact that truss members connected at a common point must have the same displacement at that point. Note that this is not the case for trusses with cross-laced members that can slide relative to one another; therefore, such designs should not be analyzed using the techniques of this study.

Each group of parallel members is characterized by one nonzero equivalent stiffness that is in the local  $x'$  direction (the member longitudinal direction). This equivalent unidirectional stiffness is determined in equation (7) for the  $n$ th group of members:

$$(C'_{1111})_n = Ev_n \quad (7)$$

where  $E$  is the Young's modulus of the truss material in the members and  $v_n$  is the volume fraction of the group of members (i.e., the ratio of the total volume of material in the members to the total volume of the truss).

The continuum stiffnesses for a truss are calculated by transforming the unidirectional stiffnesses for each of its groups of parallel members into a global coordinate system using equation (2) and by summing the results, as indicated by

$$C_{ijkl} = \sum_n (C'_{1111})_n (T_{1i}T_{1j}T_{1k}T_{1l})_n \quad (8)$$

Elements of the first row of the transformation tensor  $T_{1i}$  are simply the direction cosines between the longitudinal axis of the members and the  $i$ th coordinate axis. Therefore, equation (8) can be rewritten as

$$C_{ijkl} = \sum_n (C'_{1111})_n (\phi_i\phi_j\phi_k\phi_l)_n \quad (9)$$

where  $\phi_i$  is the  $i$ th direction cosine of the members. The continuum stiffnesses defined by equation (9) are explicit functions of the member extensional stiffnesses. These functions enable the desired continuum stiffness characteristics to be translated into member axial stiffness tailoring rules.

Equation (9) produces additional restrictions on the continuum stiffnesses of uniform trusses which should be noted. Employing the usual conversion from the matrix form of the elastic

constants to the tensor form (ref. 10), the values for the transverse and shear stiffnesses  $c_{12}$  and  $c_{66}$  are

$$c_{12} = C_{1122} = \sum_n (C'_{1111})_n (\phi_1^2 \phi_2^2)_n \quad (10)$$

$$c_{66} = C_{1212} = \sum_n (C'_{1111})_n (\phi_1^2 \phi_2^2)_n \quad (11)$$

Thus,

$$c_{12} = c_{66} \quad (12)$$

Similarly,

$$c_{13} = c_{55} \quad c_{23} = c_{44} \quad c_{45} = c_{36} \quad c_{25} = c_{46} \quad c_{14} = c_{56} \quad (13)$$

Remember that these identities must be valid for any uniform space-filling truss, regardless of its geometry, and therefore these identities should be added to those already presented in table I for all symmetry groups. Thus, under these assumptions, a generally anisotropic space-filling truss structure has only 15 independent elastic constants rather than the 21 that are normal for a generally anisotropic solid.

Trusses that are tailored to behave as isotropic continua can be characterized by two elastic constants, an equivalent continuum Young's modulus  $E_{eq}$  and an equivalent continuum Poisson's ratio  $\nu_{eq}$ . Writing the stiffnesses in equation (12) in terms of these equivalent constants gives the following condition:

$$\frac{\nu_{eq} E_{eq}}{(1 + \nu_{eq})(1 - 2\nu_{eq})} = \frac{E_{eq}}{2(1 + \nu_{eq})} \quad (14)$$

Solving equation (14) for  $\nu_{eq}$  gives the result that  $\nu_{eq}$  is equal to  $1/4$ . Therefore, any uniform three-dimensional space-filling truss structure that is globally isotropic must have an equivalent Poisson's ratio equal to  $1/4$ , and, thus, it has only one remaining independent elastic constant, which is its equivalent Young's modulus. Using a similar procedure, the two-dimensional space-filling trusses that behave isotropically must have an equivalent Poisson's ratio of  $1/3$ .

### Equivalent Stiffness-to-Density Ratio

Stiffness-to-density ratios are commonly used as indicators of the efficiency of materials. Likewise, equivalent stiffness-to-density ratios are useful indicators of the efficiency of uniform trusses. Most equivalent truss stiffness-to-density ratios are dependent on the design of the truss. However, an equivalent stiffness-to-density ratio that is only a function of the modulus-to-density ratio of the parent material will be shown to exist.

In equation (15), a sum of equivalent continuum stiffnesses for a truss is shown to be equal to the sum of the uniaxial stiffnesses of its individual groups of members. Notice that the direction cosine terms drop out because the sum of the squares of the three direction cosines for any member is equal to one.

$$\begin{aligned}
c_{11} + c_{22} + c_{33} + 2c_{23} + 2c_{13} + 2c_{12} &= C_{1111} + C_{2222} + C_{3333} + 2C_{2233} + 2C_{1133} + 2C_{1122} \\
&= \sum_n (C'_{1111})_n (\phi_1^4 + \phi_2^4 + \phi_3^4 + 2\phi_2^2\phi_3^2 + 2\phi_1^2\phi_3^2 + 2\phi_1^2\phi_2^2)_n \\
&= \sum_n (C'_{1111})_n (\phi_1^2 + \phi_2^2 + \phi_3^2)_n^2 \\
&= \sum_n (C'_{1111})_n
\end{aligned} \tag{15}$$

The equivalent density of a space-filling truss is determined by multiplying the density of the parent material  $\rho$  by the sum of the volume fractions of all groups of parallel members. Considering equation (7), this relationship can be written as

$$\rho_{\text{eq}} = \rho \sum_n v_n = \frac{\rho}{E} \sum_n (C'_{1111})_n \tag{16}$$

Dividing equation (15) by equation (16) gives the following equivalent stiffness-to-density ratio:

$$\frac{c_{11} + c_{22} + c_{33} + 2c_{23} + 2c_{13} + 2c_{12}}{\rho_{\text{eq}}} = \frac{E}{\rho} \tag{17}$$

Equation (17) is a unique relationship because it provides a direct correlation between an equivalent continuum stiffness-to-density ratio of the truss and the modulus-to-density ratio of the parent material in the truss members. Once the parent material is defined for a truss, equation (17) provides a direct relationship between the equivalent anisotropic stiffness of a truss and its equivalent density. This relationship can be used in a number of ways. For example, changes in the continuum stiffnesses because of stiffness tailoring of the truss members can be directly translated into a proportional change in the equivalent density of the truss. Similarly, requiring the sum of the continuum stiffnesses in the numerator of equation (17) to be constant during stiffness tailoring results in the equivalent density remaining constant. This requirement allows the effects of material redistribution within a truss lattice to be conveniently studied.

Equation (17) can be simplified for trusses that are tailored to be globally isotropic. Without presenting details, equation (17) reduces to the following equation by writing the equivalent continuum stiffnesses in terms of an equivalent Young's modulus and Poisson's ratio (equal to  $1/4$ ):

$$\frac{E_{\text{eq}}}{\rho_{\text{eq}}} = \frac{1}{6} \frac{E}{\rho} \tag{18}$$

The significance of equation (18) is that all uniform space-filling trusses that are globally isotropic must have the same equivalent modulus-to-density ratio regardless of their geometries or member sizes. Furthermore, this modulus-to-density ratio must be exactly  $1/6$  of the modulus-to-density ratio of the parent material.

### Equivalent Continuum Strength Tensor

The continuum strength of a truss structure is defined herein as the maximum continuum stress that the truss can sustain before any of its members buckle elastically. This failure mode, which is a local phenomenon within the truss lattice, will have one of two effects on the continuum behavior of the truss. If redundant members exist and load is redistributed, local buckling will cause a change in the continuum stiffnesses of the truss. However, if no load redistribution takes

place, local buckling will precipitate a catastrophic failure of the truss lattice. These continuum effects are analogous, respectively, to yielding and ultimate failure in a material.

Because the local failure mode in trusses can be determined analytically, a purely analytical failure theory for trusses can be constructed. In this section, a tensor that describes the strength of a truss will be constructed, and failure analysis using this strength tensor will be discussed. Having a tensor that represents the strength of a truss is advantageous because it allows strength to be readily determined in alternate reference frames or under multiaxial stress states. Material strength is not a tensor quantity, and, thus, analysis of failure in materials under multiaxial stress can be accomplished only with approximate, semiempirical theories such as that proposed by von Mises (e.g., as explained in ref. 14).

A strength tensor is constructed for trusses by converting the applied stresses into strains using the compliance equations given in equations (19) and by analyzing these strains to determine if the axial compression strain in any truss member has exceeded its critical elastic buckling limit:

$$\begin{pmatrix} \varepsilon_{11} \\ \varepsilon_{22} \\ \varepsilon_{33} \\ 2\varepsilon_{23} \\ 2\varepsilon_{13} \\ 2\varepsilon_{12} \end{pmatrix} = \begin{bmatrix} s_{11} & s_{12} & s_{13} & s_{14} & s_{15} & s_{16} \\ s_{12} & s_{22} & s_{23} & s_{24} & s_{25} & s_{26} \\ s_{13} & s_{23} & s_{33} & s_{34} & s_{35} & s_{36} \\ s_{14} & s_{24} & s_{34} & s_{44} & s_{45} & s_{46} \\ s_{15} & s_{25} & s_{35} & s_{45} & s_{55} & s_{56} \\ s_{16} & s_{26} & s_{36} & s_{46} & s_{56} & s_{66} \end{bmatrix} \begin{pmatrix} \sigma_{11} \\ \sigma_{22} \\ \sigma_{33} \\ \sigma_{23} \\ \sigma_{13} \\ \sigma_{12} \end{pmatrix} \quad (19a)$$

$$\varepsilon_{ij} = S_{ijkl}\sigma_{kl} \quad (19b)$$

Note that the compliance matrix in equation (19a) is simply the inverse of the stiffness matrix given in equation (1a). Therefore, the equivalent continuum compliances for a truss can be determined from the equivalent continuum stiffnesses derived previously.

The continuum strains, defined in tensor form in equation (19b), can be transformed into a new coordinate system described by the linear transformation tensor  $T_{ij}$ . The resulting transformed strains  $\varepsilon'_{ij}$  are

$$\varepsilon'_{ij} = T_{io}T_{jp}\varepsilon_{op} = T_{io}T_{jp}S_{opkl}\sigma_{kl} \quad (20)$$

The axial strain in any member of the truss is determined by defining an alternate coordinate system with one of its axes aligned along the longitudinal direction of the member and evaluating the normal strain along that axis. Assuming that the  $x$ -axis of the alternate coordinate system is aligned this way, the axial strain in the member is given as

$$\varepsilon'_{11} = T_{1i}T_{1j}S_{ijkl}\sigma_{kl} = \phi_i\phi_jS_{ijkl}\sigma_{kl} \quad (21)$$

where, as defined before,  $\phi_i$  is the  $i$ th direction cosine of the member.

Failure occurs in a member if its axial strain exceeds a critical value determined for elastic buckling. For the present study, the truss members are assumed to be slender and therefore to buckle as Euler columns (ref. 15); thus, the critical strain for the  $n$ th group of members is defined as

$$(\varepsilon_{\text{crit}})_n = -\pi^2 \left( \frac{r_n}{l_n} \right)^2 \quad (22)$$

where  $r_n$  is the radius of gyration and  $l_n$  is the length of the members in the  $n$ th group. The minus sign in equation (22) indicates that the critical strain is compressive. A fail-safe criterion can be constructed from equations (21) and (22) by requiring the axial strains in all members to be less than the critical value. This fail-safe criterion can be written as

$$\left[ \frac{(\phi_i \phi_j)_n S_{ijkl}}{-\pi^2 \left(\frac{r_n}{l_n}\right)^2} \right] \sigma_{kl} = [\Omega_{kl}]_n \sigma_{kl} \leq 1 \quad (23)$$

The bracketed term in equation (23) can either be thought of as a third-order tensor representing the strength of the truss or as a collection of second-order tensors, each representing the strength of a group of parallel members within the truss. The product of this strength tensor and the second-order applied stress tensor  $\sigma_{kl}$  is a vector of constants, one for each of the groups of parallel members. For elastic failure to occur, any one of these constants must be  $\geq 1$ . Thus, the critical stress at which failure occurs is the minimum stress at which one or more of these constants is equal to 1.

Equation (23) represents a purely analytical failure theory for space-filling trusses which can be used with equal ease to analyze strength under multiaxial or uniaxial loading. Similarly, strength in alternate coordinate systems can be readily handled by simply transforming the collection of second-order strength tensors  $\Omega_{kl}$  in the same way that a stress or strain tensor would be transformed.

Equation (23) can be used, as described, to determine the strength of a given truss design. Additionally, this equation is useful for tailoring the strength of a truss design because it is an explicit relationship between the strength of individual members (i.e.,  $r_n/l_n$ ) and the continuum strength of the truss. Strength tailoring is accomplished by varying the strength of individual members to effect a desired change in the continuum strength of the truss. Note that because the continuum compliances of the truss appear in equation (23), strength tailoring is not independent of stiffness tailoring. Consequently, tailoring the continuum stiffnesses of a truss also will change its continuum strength characteristics.

In the remaining sections of this paper, examples of stiffness and strength tailoring of uniform trusses are presented. Truss geometries are selected for analytical simplicity, thus allowing emphasis to be placed on developing an understanding of the analysis techniques.

## Examples of Stiffness and Strength Tailoring in Trusses

Equations (9), (17), and (23) provide the basis for analysis of the continuum stiffness, density, and strength of uniform space-filling truss structures. By providing explicit relationships between these continuum quantities and truss design parameters, these equations are effective tools that enable efficient tailoring of the truss stiffness and strength characteristics. In this section, these equations are applied to the analysis of two commonly used truss geometries and to the tailoring of designs that have continuum isotropic and orthotropic behaviors.

### Regular Octahedral Truss

The octahedral truss (also known as the tetrahedral truss, ref. 2, or the octet truss) is a common geometry that derives its name from its members that connect to form octahedrons and tetrahedrons. For the present study, a regular octahedral truss is considered which has all identical members. A repeating cell from this truss is shown in figure 3. The cell contains a regular octahedron at its center (fig. 3(a)) and tetrahedrons connected to each of the eight faces of the octahedron (fig. 3(b)). Space is filled by translational replication of this cell in each of the three coordinate directions.

Because all members are identical, the octahedral truss has digonal symmetry axes along the lines  $x = y$ ,  $x = z$ , and  $y = z$ ; trigonal symmetry axes along the lines  $x = y = z$ ,  $-x = y = z$ ,  $x = -y = z$ , and  $x = y = -z$ ; and quadragonal symmetry axes along the  $x$ -,  $y$ -, and  $z$ -axes. This combination of symmetry axes indicates that the regular octahedral truss is a member of rotational symmetry group  $j$ .

**Calculation of continuum stiffness and density.** In table I, the behavior of the regular octahedral truss is characterized by the three independent elastic constants  $c_{11}$ ,  $c_{12}$ , and  $c_{66}$ . Equation (12) further reduces this number to two. However, these constants lack the relationship  $c_{66} = (c_{11} - c_{12})/2$ ; thus, the regular octahedral truss is not globally isotropic. Values for the elastic constants can be determined from equations (7) and (9). Six different groups of parallel members exist in the octahedral truss, and all members are identical and assumed to have a cross-sectional area of  $A$ . With the half-height of the regular octahedron defined to be  $L$ , as shown in figure 3, the length of each of the members is  $\sqrt{2}L$ . Then, the equivalent unidirectional stiffness for each of the six groups of parallel members is

$$(C'_{1111})_n = \frac{EA}{\sqrt{2}L^2} \quad (24)$$

Substituting equation (24) into equation (9) along with the appropriate direction cosines for the different member groups, gives the result presented in equation (25) for the equivalent continuum stiffness matrix of the octahedral truss:

$$[c_{mn}] = \frac{EA}{2\sqrt{2}L^2} \begin{bmatrix} 2 & 1 & 1 & 0 & 0 & 0 \\ 1 & 2 & 1 & 0 & 0 & 0 \\ 1 & 1 & 2 & 0 & 0 & 0 \\ 0 & 0 & 0 & 1 & 0 & 0 \\ 0 & 0 & 0 & 0 & 1 & 0 \\ 0 & 0 & 0 & 0 & 0 & 1 \end{bmatrix} \quad (25)$$

Notice that the continuum stiffnesses obey the restrictions in table I and equation (12).

Because all members in the regular octahedral truss are identical, the relative magnitudes of the continuum stiffnesses for the octahedral truss are constrained by the proportions given in the matrix of equation (25). Therefore, changing the axial stiffness of the truss members can only uniformly change all continuum stiffnesses.

The equivalent density of the octahedral truss can be calculated by substituting the stiffnesses from equation (25) into equation (17). Rearranging and simplifying gives

$$\rho_{eq} = \frac{3\sqrt{2}\rho A}{L^2} \quad (26)$$

**Calculation of continuum strength.** Before applying equation (23) to calculate the continuum strength of the octahedral truss, the tensor form of the continuum compliances must be determined from the stiffness matrix given in equation (25). This process is done by inverting the stiffness matrix to get the compliance matrix and then employing the usual conversion from matrix form to tensor form on the individual compliances (ref. 10). The only remaining unknown truss parameter is the radius of gyration of its members.

Suppose that the strength of the octahedral truss under a continuum uniaxial compression is required. Assuming this stress to have magnitude  $\sigma_{\text{ult}}$  and to be applied along a vector given by the spherical coordinates  $\theta$  and  $\varphi$  (as shown in fig. 4), the applied continuum stress tensor can be written as

$$[\sigma_{kl}] = -\sigma_{\text{ult}} \begin{bmatrix} (\sin^2 \theta \cos^2 \varphi) & (\sin^2 \theta \sin \varphi \cos \varphi) & (\sin \theta \cos \theta \cos \varphi) \\ (\sin^2 \theta \sin \varphi \cos \varphi) & (\sin^2 \theta \sin^2 \varphi) & (\sin \theta \cos \theta \sin \varphi) \\ (\sin \theta \cos \theta \cos \varphi) & (\sin \theta \cos \theta \sin \varphi) & (\cos^2 \theta) \end{bmatrix} \quad (27)$$

The compression strength is determined by substituting equation (27) into equation (23). After simplification, equation (23) reduces to a set of six scalar equations ( $n = 1$  to 6), one for each group of parallel members in the truss. Each of these equations can be solved for the value of  $\sigma_{\text{ult}}$  which is necessary to cause Euler buckling in the corresponding member. The minimum value of  $\sigma_{\text{ult}}$  determined from these six equations is the lowest uniaxial compression stress at which local buckling occurs within the truss lattice. This value is defined as the uniaxial compression strength for the given set of  $\theta$  and  $\varphi$ .

A three-dimensional plot of the uniaxial compression strength of the octahedral truss is presented in figure 4 for a range of  $\theta$  and  $\varphi$  from  $0^\circ$  to  $90^\circ$ . Because of symmetry, the strength in all other quadrants is identical. A factor of 2 variation exists in the compression strength of the lattice, and, not surprisingly, the directions of minimum strength are coincident with the directions of the members of the truss. Maximum strength occurs for loading along the three coordinate axes and along the line  $x = y = z$ . The value of the minimum strength is

$$\sigma_{\text{ult}} = \frac{EA\pi^2 r^2}{2\sqrt{2}L^4} \quad (28)$$

Because all members are identical, changing the strength of the members would change the vertical scale of the strength plot given in figure 4, but it would not change its shape. Introducing member-specific properties will alter the equivalent continuum stiffness and strength; however, this would destroy the geometric symmetry of the lattice and introduce additional independent stiffnesses. In the following section, a truss based on the octahedral lattice is designed for isotropic stiffness and nearly isotropic strength.

### Isotropic Warren Truss

The lattice of the regular octahedral truss is modified by adding members that connect all six vertices of each octahedron to the geometric center of the octahedron, as shown in figure 5(a). The resulting arrangement of new members forms a cubic lattice within the octahedral lattice, with the edges of the cube lying parallel to the three coordinate axes and each cube containing a regular tetrahedron, as shown in figure 5(b). The members of the cubic lattice are of length  $L$ , whereas the members of the original octahedral lattice are of length  $\sqrt{2}L$ . This truss geometry is often referred to as the Warren truss because its lattice arrangement is similar to that of a common two-dimensional truss of the same name. Similar to the regular octahedral truss, the Warren truss is a member of symmetry group  $j$ , and it has two independent elastic constants  $c_{11}$  and  $c_{12}$ . However, unlike the octahedral truss, the Warren truss has two different members whose relative stiffnesses and strengths can be tailored to affect the continuum behavior of the truss without violating its geometric and elastic symmetry. In this section, it is demonstrated that the continuum strength and stiffness properties of the lattice can be tailored by redistributing material within the truss lattice. The material is transferred from the octahedral lattice members

to the cubic lattice members so that the continuum stiffnesses become isotropic. Also, the relative strengths of the members are tailored to reduce variations in continuum compression strength.

**Continuum stiffness tailoring.** The Warren truss is composed of nine different groups of parallel members. Three groups correspond to the cubic lattice, and six groups correspond to the octahedral lattice. The continuum stiffnesses for the Warren truss can be determined by adding the contributions because of the cubic lattice members to the result presented in equation (25) for the octahedral lattice. The cross-sectional areas of the members in the cubic lattice and the octahedral lattice are defined to be  $A_c$  and  $A_o$ , respectively. Thus, the equivalent uniaxial stiffnesses of the three groups of parallel cubic lattice members are given by

$$(C'_{1111})_n = \frac{EA_c}{L^2} \quad (29)$$

Substituting equation (29) into equation (9), along with the appropriate direction cosines, and adding the result to that presented in equation (25) gives

$$[c_{mn}] = \frac{EA_o}{2\sqrt{2}L^2} \begin{bmatrix} 2 + 2\sqrt{2}\delta_c & 1 & 1 & 0 & 0 & 0 \\ 1 & 2 + 2\sqrt{2}\delta_c & 1 & 0 & 0 & 0 \\ 1 & 1 & 2 + 2\sqrt{2}\delta_c & 0 & 0 & 0 \\ 0 & 0 & 0 & 1 & 0 & 0 \\ 0 & 0 & 0 & 0 & 1 & 0 \\ 0 & 0 & 0 & 0 & 0 & 1 \end{bmatrix} \quad (30)$$

where  $\delta_c$  is defined as  $A_c/A_o$ . If  $\delta_c$  is equal to 0, the cross-sectional area of the cubic lattice members is 0, and equation (30) is identical to equation (25). As before, an equivalent density can be calculated using equation (17) and the stiffnesses presented in equation (30). The result is

$$\rho_{\text{eq}} = \frac{(3\sqrt{2} + 3\delta_c)\rho A_o}{L^2} \quad (31)$$

To study the effects of redistribution of material within the truss, the total amount of material must remain constant. For convenience, the density of the Warren truss is required to be the same as that of the regular octahedral truss by setting equation (26) equal to equation (31). The result is

$$A_o = \frac{A}{1 + \delta_c/\sqrt{2}} \quad (32)$$

where  $A$  is the cross-sectional area of the members in the regular octahedral truss that was analyzed previously. Equation (32) defines the relation between the cross-sectional areas of the cubic and octahedral lattice members within the Warren truss; this relation must be valid to keep the equivalent density of the Warren truss equal to that of the regular octahedral truss. Substituting equation (32) into equation (30) gives explicit equations for the continuum stiffnesses of the Warren truss in terms of the member area ratio  $\delta_c$ . To better understand the effects of redistribution of material, the stiffness components in equation (30) are translated into equivalent Young's modulus, Poisson's ratio, and shear modulus, as follows:

$$E_{\text{eq}} = \frac{(c_{11} + 2c_{12})(c_{11} - c_{12})}{c_{11} + c_{12}} = \frac{4EA(1 + 2\sqrt{2}\delta_c)}{2\sqrt{2}L^2(3 + 2\sqrt{2}\delta_c)} \quad (33)$$

$$\nu_{\text{eq}} = \frac{c_{12}}{c_{11} + c_{12}} = \frac{1}{3 + 2\sqrt{2}\delta_c} \quad (34)$$

$$G_{\text{eq}} = c_{66} = \frac{EA}{2\sqrt{2}L^2(1 + \delta_c/\sqrt{2})} \quad (35)$$

These stiffness components are plotted in figure 6 as functions of the area ratio  $\delta_c$ . For  $\delta_c = 0$ , no material has been redistributed from the octahedral lattice to the cubic lattice, and the stiffnesses represent those of the octahedral truss. As  $\delta_c$  is increased, material is moved from the octahedral lattice to the cubic lattice, and this process is accompanied by an increase in the equivalent Young's modulus and decreases in the equivalent Poisson's ratio and the equivalent shear modulus. As seen from equations (34) and (35), when  $\delta_c$  becomes large, both the Poisson's ratio and the shear modulus approach 0. This effect is consistent with the fact that the cubic lattice of members is not a kinematically stable truss by itself. Because of this, considering designs with very large values of  $\delta_c$  is unreasonable.

For the Warren truss to be globally isotropic, the stiffnesses must satisfy the following condition:

$$G_{\text{eq}} = \frac{E_{\text{eq}}}{2(1 + \nu_{\text{eq}})} \quad (36)$$

Substituting the expressions from equations (33) to (35) into equation (36) shows that  $\delta_c$  must be equal to  $1/(2\sqrt{2})$  for isotropy. Substituting this value of  $\delta_c$  into equation (32) gives a value of  $4A/5$  for the cross-sectional area of the members in the octahedral lattice and, consequently, a value of  $\sqrt{2}A/5$  for the cross-sectional area of the members in the cubic lattice. Thus, if  $1/5$  of the material that was originally in the members of the octahedral truss is redistributed into the members of the cubic lattice, the resulting truss behaves isotropically. The isotropic values for the equivalent Young's modulus, Poisson's ratio, and shear modulus are

$$(E_{\text{eq}})_{\text{iso}} = \frac{EA}{\sqrt{2}L^2} \quad (\nu_{\text{eq}})_{\text{iso}} = \frac{1}{4} \quad (G_{\text{eq}})_{\text{iso}} = \frac{\sqrt{2}EA}{5L^2} \quad (37)$$

Notice that the equivalent isotropic Poisson's ratio is  $1/4$ , which is the value that was predicted earlier for globally isotropic trusses. Also, calculating the ratio of the equivalent isotropic Young's modulus (eq. (37)) to the equivalent density (eq. (26)) gives the result predicted in equation (18) for globally isotropic trusses.

**Continuum strength tailoring.** Applying the same procedure used for the octahedral truss, the continuum strength of the isotropic Warren truss can be determined and the effects on continuum strength of varying the strength of the truss members can be evaluated. For comparison, the same continuum stress tensor given in equation (27) is also applied to the Warren truss. Two cases are analyzed. In the first case, all members in the truss are assumed to have the same radius of gyration, and in the second case, all members are assumed to have the same buckling load. The first case is representative of a truss with thin-walled members of equal cross-sectional diameter. The second case illustrates the effects of tailoring individual member buckling strengths on the continuum strength of the truss.

For the first case, the radius of gyration of all members is  $r$ , and the lengths of the members are  $L$  for the cubic lattice and  $\sqrt{2}L$  for the octahedral lattice. These values, the continuum compliances determined from equation (30), and the appropriate direction cosines are substituted into equation (23). The result is a set of nine scalar equations, one for each group of parallel

members in the truss, from which the minimum value of  $\sigma_{\text{ult}}$  is determined for the given set of  $\theta$  and  $\varphi$ .

A three-dimensional plot of the uniaxial compression strength of the isotropic Warren truss is presented in figure 7 for the same range of  $\theta$  and  $\varphi$  as in figure 4. The shape of the strength plot is similar to that of the octahedral truss, and, despite the redistribution of material from the octahedral lattice, the values and the directions of the minimum and maximum strength are the same as those for the octahedral truss. The directions and maximum strength are coincident with the directions of the cubic lattice members, and the directions of minimum strength are coincident with the directions of the octahedral lattice members. Requiring that all members have the same radius of gyration causes the cubic lattice members to have twice the buckling load of the octahedral lattice members because of the difference in their lengths. This effect causes a factor of 2 variation in the continuum strength.

Variation in truss strength might not be a concern for many design applications; however, if it is desirable to have a truss that behaves isotropically in stiffness, it is probably also desirable for the truss to behave isotropically in strength. By tailoring the buckling loads of the cubic lattice members to be the same as those of the octahedral lattice, the variations in continuum strength can be significantly reduced. For this case, the radius of gyration of the cubic lattice members is reduced to  $r/\sqrt{2}$  so that the buckling loads of all members are the same. A plot of the resulting continuum compression strength is presented in figure 8. Although some variation still exists in the continuum strength, the magnitude of the variation has been significantly reduced.

The use of three-dimensional strength plots is particularly helpful for developing strength tailoring rules because these plots provide visualization of the correlation between member orientations and continuum strength variations. Without this correlation, developing strength tailoring rationale for the members would be difficult. The example presented is fairly simple because of the isotropic stiffness behavior and geometric symmetry of the Warren truss. Therefore, the correlation between variations in continuum strength and the orientation of members is fairly obvious. However, for trusses with less geometric symmetry or more complex applied stress tensors, this correlation might not be apparent without the use of a three-dimensional strength plot.

### Orthotropic Warren Truss

Many applications exist for large truss structures with orthotropic, rather than isotropic, continuum properties. For orthotropic applications, the requirements on continuum stiffness and strength are much higher in one direction than in others. For example, many applications involve beam-like trusses that primarily carry bending and torsional loads. In these cases, the longitudinal (along the length of the beam) stiffness and strength requirements are much higher than the transverse stiffness and strength requirements. Therefore, using a truss with orthotropic continuum properties is probably more efficient than using one with isotropic properties.

Table I shows that trusses of symmetry groups  $i$  and  $j$  are not candidates for orthotropic design because their stiffnesses (and strengths) must be the same in all three coordinate directions. Trusses of all other symmetry groups are candidates for orthotropic tailoring because their properties in the  $z$  direction can differ from those in either the  $x$  or the  $y$  direction. The truss presented in figure 9 is a variation of the Warren truss design that is a member of symmetry group  $f$  and is, thus, a possible candidate for orthotropic design. The lattice arrangement of this truss is identical to that of the Warren truss except the length of the repeating cell in the  $z$  direction differs from that in either the  $x$  or the  $y$  directions by the proportion  $\beta$ . This section will show the results of applying stiffness and strength tailoring techniques to generate orthotropic designs that have high stiffnesses and strengths in the  $z$  direction but which have the same equivalent density as that of the isotropic Warren truss.

**Calculation of continuum stiffnesses.** The orthotropic Warren truss shown in figure 9 has four different members. The cross-sectional areas for members of groups 1 and 2 are defined as  $\delta_1 A$  and  $\delta_2 A$ , respectively, where  $\delta_1$  and  $\delta_2$  are variable area ratios and  $A$  is the cross-sectional area assumed earlier for the members in the octahedral truss. The equivalent uniaxial stiffnesses for groups of these members are determined using equation (7), and the results are given in equations (38) and (39):

$$(C'_{1111})_1 = \frac{\delta_1 EA}{L^2} \quad (38)$$

$$(C'_{1111})_2 = \frac{\delta_2 EA(1 + \beta^2)^{1/2}}{2\beta L^2} \quad (39)$$

For simplicity, members of groups 3 and 4 are assumed to be the same as those in the isotropic Warren truss. Therefore, the cross-sectional area of members of group 3 is  $\sqrt{2}A/5$ , and the cross-sectional area of members of group 4 is  $4A/5$ . The equivalent uniaxial stiffnesses are the same for member groups 1 and 2, and the value of this stiffness is given in equation (40):

$$(C'_{1111})_3 = (C'_{1111})_4 = \frac{\sqrt{2}EA}{5\beta L^2} \quad (40)$$

Substituting these uniaxial stiffnesses and the appropriate transformation tensors into equation (9) and simplifying gives the following values for the nonzero continuum stiffnesses:

$$c_{11} = c_{22} = \frac{EA}{\beta L^2} \left[ \frac{2\sqrt{2}}{5} + \frac{\delta_2}{(1 + \beta^2)^{3/2}} \right] \quad (41)$$

$$c_{12} = c_{66} = \frac{\sqrt{2}EA}{5\beta L^2} \quad (42)$$

$$c_{13} = c_{23} = c_{44} = c_{55} = \frac{EA}{\beta L^2} \left[ \frac{\beta^2 \delta_2}{(1 + \beta^2)^{3/2}} \right] \quad (43)$$

$$c_{33} = \frac{EA}{\beta L^2} \left[ \delta_1 \beta + \frac{2\beta^4 \delta_2}{(1 + \beta^2)^{3/2}} \right] \quad (44)$$

Note that these stiffnesses obey the conditions presented in table I and equations (12) and (13) for trusses of symmetry group  $f$ . Equations (41) through (44) are explicit functions of the three remaining design parameters  $\beta$ ,  $\delta_1$ , and  $\delta_2$ . Therefore, these equations can be used directly to determine how variations in the design parameters affect the orthotropic characteristics of the truss.

An equivalent density can be calculated for the orthotropic Warren truss by substituting the stiffnesses from equations (41) through (44) into equation (17). The result is

$$\rho_{eq} = \frac{\rho A}{\beta L^2} \left[ \frac{6\sqrt{2}}{5} + \delta_1 \beta + 2(1 + \beta^2)^{1/2} \delta_2 \right] \quad (45)$$

Setting equation (45) equal to equation (26) ensures that the equivalent density of the orthotropic Warren truss is the same as that of the regular octahedral truss and the isotropic Warren truss. The resulting expression can be rearranged to give the following condition on the area ratio  $\delta_2$ :

$$\delta_2 = \frac{(3\sqrt{2} - \delta_1)\beta - 6\sqrt{2}/5}{2(1 + \beta^2)^{1/2}} \quad (46)$$

Equation (46) reduces the set of independent design parameters to the repeating cell length ratio  $\beta$  and the cross-sectional area ratio  $\delta_1$ .

An equivalent  $z$ -direction Young's modulus can be determined for the orthotropic Warren truss by inverting the  $s_{33}$  component of the compliance matrix as follows:

$$(E_{\text{eq}})_z = \frac{1}{s_{33}} \quad (47)$$

Performing this calculation gives the result

$$(E_{\text{eq}})_z = \frac{\sqrt{2}EA [15\delta_1/\sqrt{2} + 18\beta^3 - 5(\delta_1/\sqrt{2} - 6\beta/5)^2]}{L^2(15 - 5\delta_1/\sqrt{2} + 12\beta + 6\beta^3)} \quad (48)$$

To determine the improvement in stiffness in the  $z$  direction, the modulus given in equation (48) is divided by the Young's modulus of the isotropic Warren truss given in equation (37). The resulting normalized  $z$ -direction Young's modulus is

$$\frac{(E_{\text{eq}})_z}{(E_{\text{eq}})_{\text{iso}}} = \frac{30\delta_1/\sqrt{2} + 36\beta^3 - 10(\delta_1/\sqrt{2} - 6\beta/5)^2}{15 - 5\delta_1/\sqrt{2} + 12\beta + 6\beta^3} \quad (49)$$

A three-dimensional plot of the normalized  $z$ -direction Young's modulus is presented in figure 10 for ranges of  $\beta$  and  $\delta_1$ . The isotropic Warren truss is characterized by  $\delta_1 = \sqrt{2}/5$  and  $\beta = 1$ ; this point on the plot corresponds to a normalized  $z$  modulus equal to 1. As  $\delta_1$  increases, for a fixed value of  $\beta$ , the material transfers from members of group 2 to members of group 1 (see fig. 9). This material transfer causes an increase in the  $z$  modulus because the group 1 members are oriented parallel to the  $z$  direction. As  $\beta$  increases, for a fixed value of  $\delta_1$ , the number of group 3 and group 4 members in a given volume decreases. To maintain constant density, material is redistributed among group 1 and group 2 members, thus also causing an increase in the  $z$  modulus.

**Calculation of continuum  $z$ -direction strength.** The strength of the orthotropic Warren truss is calculated for a uniform continuum compression applied in the  $z$  direction. This applied stress tensor is given in equation (50) and is substituted into equation (23):

$$[\sigma_{kl}] = \begin{bmatrix} 0 & 0 & 0 \\ 0 & 0 & 0 \\ 0 & 0 & -(\sigma_{\text{ult}})_z \end{bmatrix} \quad (50)$$

Because their alignment is parallel to the  $z$  direction, members in group 1 buckle at lower continuum stresses than the remaining members in the truss. (This result was verified through

additional analysis not presented herein.) Thus, considering only buckling in group 1 members, equation (23) can be reduced to equation (51), where  $r_1$  and  $l_1$  are the radius of gyration and length of members in group 1:

$$(\sigma_{\text{ult}})_z = \frac{\pi^2 r_1^2}{l_1^2 s_{33}} \quad (51)$$

Defining the radius of gyration of these members to be  $r$  and their length to be  $\beta L$  (see fig. 9) and substituting the result from equation (47) gives the following expression for the  $z$ -direction compression strength of the orthotropic Warren truss:

$$(\sigma_{\text{ult}})_z = \frac{\pi^2 r^2}{\beta^2 L^2} (E_{\text{eq}})_z \quad (52)$$

The  $z$ -direction compression strength of the isotropic Warren truss can be determined from figure 7 ( $\theta = 0^\circ$ ), and this value can be used to normalize equation (52). The result is

$$\frac{(\sigma_{\text{ult}})_z}{(\sigma_{\text{ult}})_{\text{iso}}} = \frac{(E_{\text{eq}})_z}{\beta^2 (E_{\text{eq}})_{\text{iso}}} \quad (53)$$

Unlike the  $z$  modulus, the factor of  $\beta^2$  in the denominator of equation (53) causes the  $z$ -direction strength to decrease with increasing  $\beta$ . However, it is apparent that both modulus and strength have the same variation with  $\delta_1$ . A three-dimensional plot of the normalized  $z$ -direction compression strength is presented in figure 11 for comparison with the modulus plot in figure 10. Because both modulus and strength increase as  $\delta_1$  increases, selecting the largest practical value for  $\delta_1$  is best. As an example, if the cross-sectional areas of all members within the truss are constrained so that they differ by no more than a factor of 5, the maximum allowable value for  $\delta_1$  would be  $\sqrt{2}$ . Assuming this value for  $\delta_1$  gives the following for all the member cross-sectional areas:

$$A_1 = \sqrt{2}A \quad A_2 = \frac{(10\beta - 6)A}{5(2 + 2\beta^2)^{1/2}} \quad A_3 = \sqrt{2}A/5 \quad A_4 = 4A/5 \quad (54)$$

A plot of the normalized  $z$ -direction strength and modulus is presented in figure 12, assuming  $\delta_1$  is equal to  $\sqrt{2}$ . As explained, extending the length of the Warren truss cell in the  $z$  direction (increasing  $\beta$ ) increases the stiffness while decreasing the strength of the truss. Therefore, the optimum length for the truss cell depends on the relative importance of continuum strength and continuum stiffness in the design.

## Concluding Remarks

A deterministic procedure has been presented for tailoring the continuum stiffness and strength of uniform space-filling truss structures through the appropriate selection of truss geometry and member sizes (i.e., flexural and axial stiffnesses and length). A key aspect of this procedure is symbolic manipulation of the equivalent continuum constitutive equations to produce explicit relationships between truss member sizes and continuum strength and stiffness. To help select an appropriate truss geometry for a given application, a finite set of possible geometric symmetry groups which characterize uniform trusses has been presented, and the implied elastic symmetry associated with each geometric symmetry group has been identified.

Equivalent continuum stiffness has been determined using an existing technique assuming that the displacement field within a truss is single-valued and the members within a truss carry only axial load. Based on these assumptions, generally anisotropic trusses are shown

to be characterized by 18 independent elastic constants rather than 21 as is normal for a generally anisotropic solid. This result guarantees that all three-dimensional trusses that behave isotropically, in a continuum sense, must have an equivalent Poisson's ratio of  $1/4$ . Furthermore, a direct relationship was derived between an anisotropic stiffness-to-density ratio of a truss and the stiffness-to-density ratio of its parent material. Using this relationship, the equivalent Young's modulus-to-density ratio of any isotropic three-dimensional truss is shown to be exactly  $1/6$  times the modulus-to-density ratio of the parent material of the truss.

A purely analytical failure theory has been developed for trusses by defining failure as the elastic buckling of any member within the truss lattice. This theory allows the construction of a strength tensor that simplifies failure analysis under multiaxial stress and alternate coordinate systems.

To illustrate the application of these analysis techniques, truss designs have been developed which behave isotropically and orthotropically under continuum loading. In these examples, stiffness tailoring has been accomplished through redistribution of material among the truss members, and strength tailoring has been accomplished by varying the relative buckling strengths of the members. This deterministic approach to the analysis and tailoring of truss behavior can significantly enhance the understanding of relationships between the design parameters and the continuum elastic behavior of trusses. Ultimately, this improved understanding should enable the creation of more efficient truss designs.

NASA Langley Research Center  
Hampton, VA 23665-5225  
March 6, 1992

## References

1. Barclay, D. L.; Brogren, E. W.; Fosth, D. C.; Gates, R. M.; and Straayer, J. W.: *Large Space Structures - Configuration, Packaging, and Response Studies*. NASA CR-158928, 1978.
2. Mikulas, Martin M., Jr.; Bush, Harold G.; and Card, Michael F.: *Structural Stiffness, Strength and Dynamic Characteristics of Large Tetrahedral Space Truss Structures*. NASA TM X-74001, 1977.
3. Boyer, William J., compiler: *Large Space Antenna Systems Technology 1984*. NASA CP-2368, 1985.
4. Noor, Ahmed K.; and Mikulas, Martin M., Jr.: *Continuum Modeling of Large Lattice Structures - Status and Projections*. NASA TP-2767, 1988.
5. Wolfram, Stephen: *Mathematica™ -- A System for Doing Mathematics by Computer*. Addison Wesley Publ. Co., Inc., c.1988.
6. Mikulas, Martin M., Jr.; Wright, Andrew S., Jr.; Bush, Harold G.; Watson, Judith J.; Dean, Edwin B.; Twigg, Leonard T.; Rhodes, Marvin D.; Cooper, Paul A.; Dorsey, John T.; Lake, Mark S.; Young, John W.; Stein, Peter A.; Housner, Jerrold M.; and Ferebee, Melvin J., Jr.: *Deployable/Erectable Trade Study for Space Station Truss Structures*. NASA TM-87573, 1985.
7. Cracknell, Arthur P.: *Crystals and Their Structures*. Pergamon Press, Inc., c.1969.
8. Buerger, Martin J.: *Contemporary Crystallography*. McGraw-Hill, Inc., c.1970.
9. Love, A. E. H.: *A Treatise on the Mathematical Theory of Elasticity, Fourth ed.* Dover Publ., Inc., 1944.
10. Lekhnitskii, S. G.: *Theory of Elasticity of an Anisotropic Body*. Mir Publ. (Moscow), 1981.
11. Rosen, B. Walter; and Shu, Larry S.: On Some Symmetry Conditions for Three Dimensional Fibrous Composites. *J. Compos. Mater.*, vol. 5, Apr. 1971, pp. 279-282.
12. Nayfeh, Adnan H.; and Hefzy, Mohamed S.: Continuum Modeling of Three-Dimensional Truss-Like Space Structures. *AIAA J.*, vol. 16, no. 8, Aug. 1978, pp. 779-787.
13. Jones, Robert M.: *Mechanics of Composite Materials*. McGraw-Hill Book Co., c.1975.

14. Hellan, Kåre: *Introduction to Fracture Mechanics*. McGraw-Hill, Inc., c.1984.
15. Timoshenko, Stephen P.; and Gere, James M.: *Theory of Elastic Stability, Second ed.* McGraw-Hill Book Co., 1961.

Table I. Elastic Characteristics of Rotational Symmetry Groups

Rotational symmetry group <sup>a</sup>	Conditions on continuum stiffnesses	Independent elastic constants
No symmetry	None	21
<i>a</i>	$c_{14}, c_{15}, c_{24}, c_{25}, c_{34}, c_{35}, c_{46}, c_{56} = 0$	13
<i>b</i>	Same as group <i>a</i> with $c_{16}, c_{26}, c_{36}, c_{45} = 0$	9
<i>c</i>	$c_{16}, c_{26}, c_{34}, c_{35}, c_{36}, c_{45} = 0$ ; $c_{11} = c_{22}$ ; $c_{44} = c_{55}$ ; $c_{13} = c_{23}$ ; $c_{14} = -c_{24} = c_{56}$ ; $c_{15} = -c_{25} = -c_{46}$ ; $c_{66} = (c_{11} - c_{12})/2$	7
<i>d</i>	Same as group <i>c</i> with $c_{15}, c_{25}, c_{46} = 0$	6
<i>e</i>	Same as group <i>a</i> with $c_{36}, c_{45} = 0$ ; $c_{11} = c_{22}$ ; $c_{44} = c_{55}$ ; $c_{13} = c_{23}$ ; $c_{16} = -c_{26}$	7
<i>f</i>	Same as group <i>e</i> with $c_{16}, c_{26} = 0$	6
<i>g</i>	Same as group <i>c</i> with $c_{14}, c_{15}, c_{24}, c_{25}, c_{46}, c_{56} = 0$	5
<i>h</i>	Same as group <i>g</i>	5
<i>i</i>	Same as group <i>b</i> with $c_{11} = c_{22} = c_{33}$ ; $c_{12} = c_{13} = c_{23}$ ; $c_{44} = c_{55} = c_{66}$	3
<i>j</i>	Same as group <i>i</i>	3

<sup>a</sup>See figure 2.

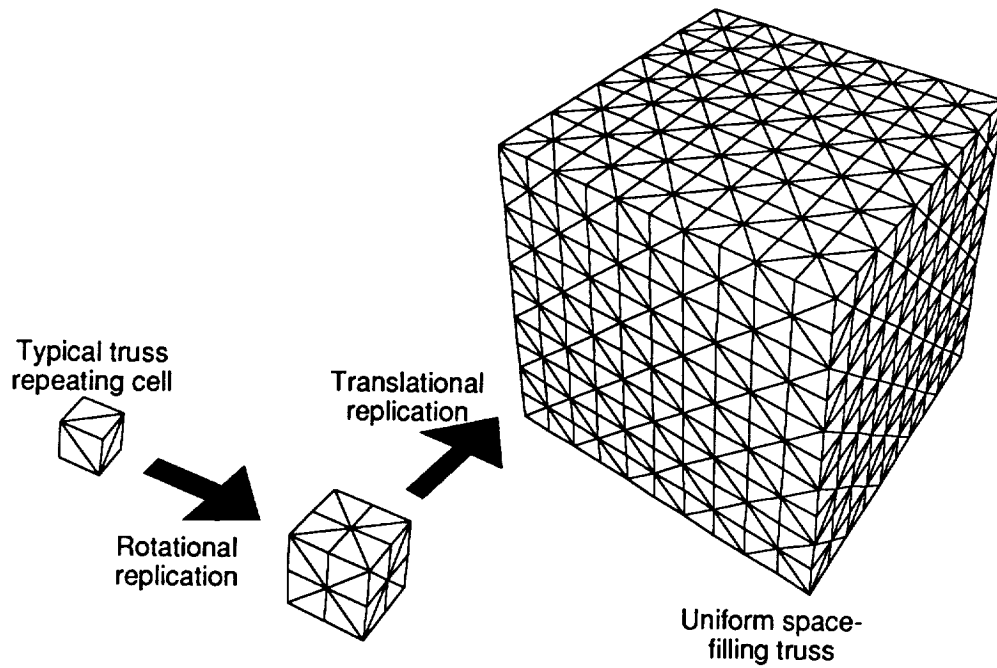


Figure 1. Large uniform trusses generated from repeating cell.

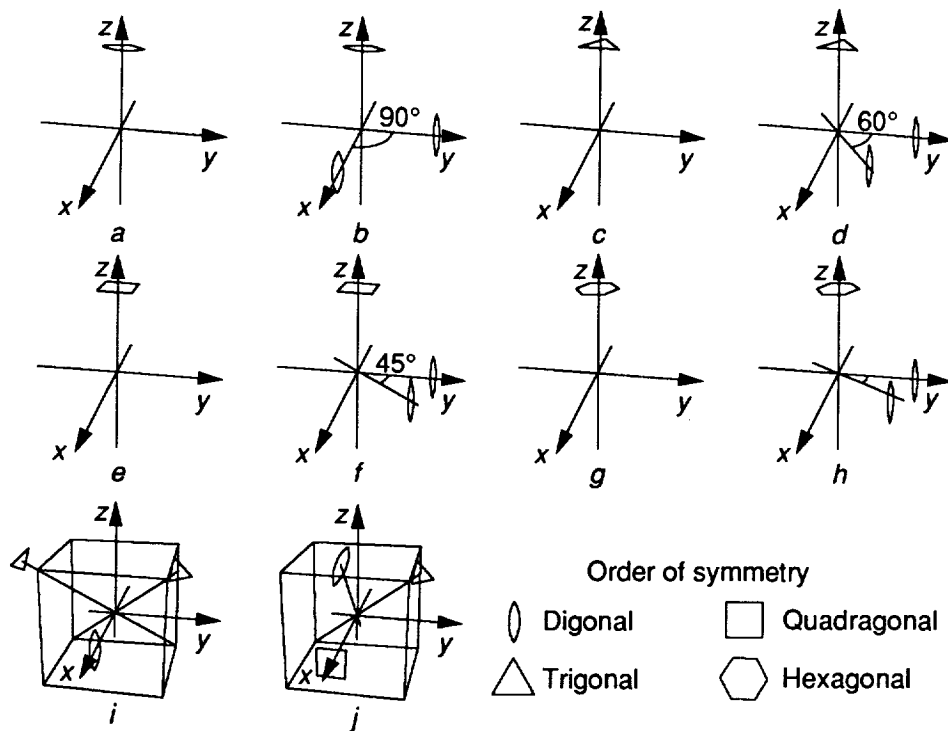
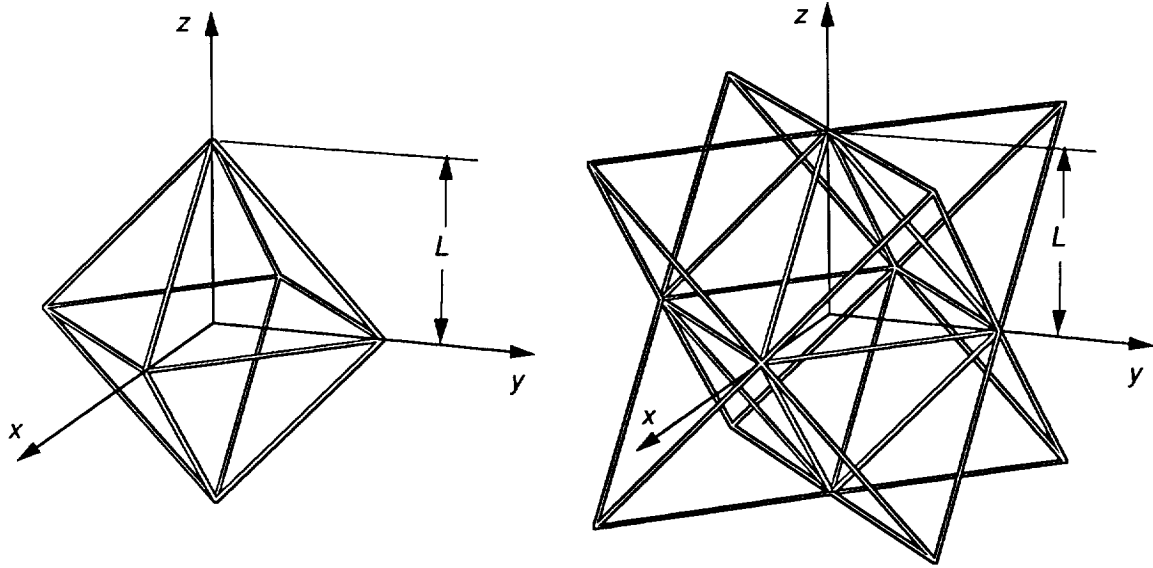


Figure 2. Possible rotational symmetry groups.



(a) Regular octahedron.

(b) Complete repeating cell with regular tetrahedron.

Figure 3. Repeating cell for regular octahedral truss.

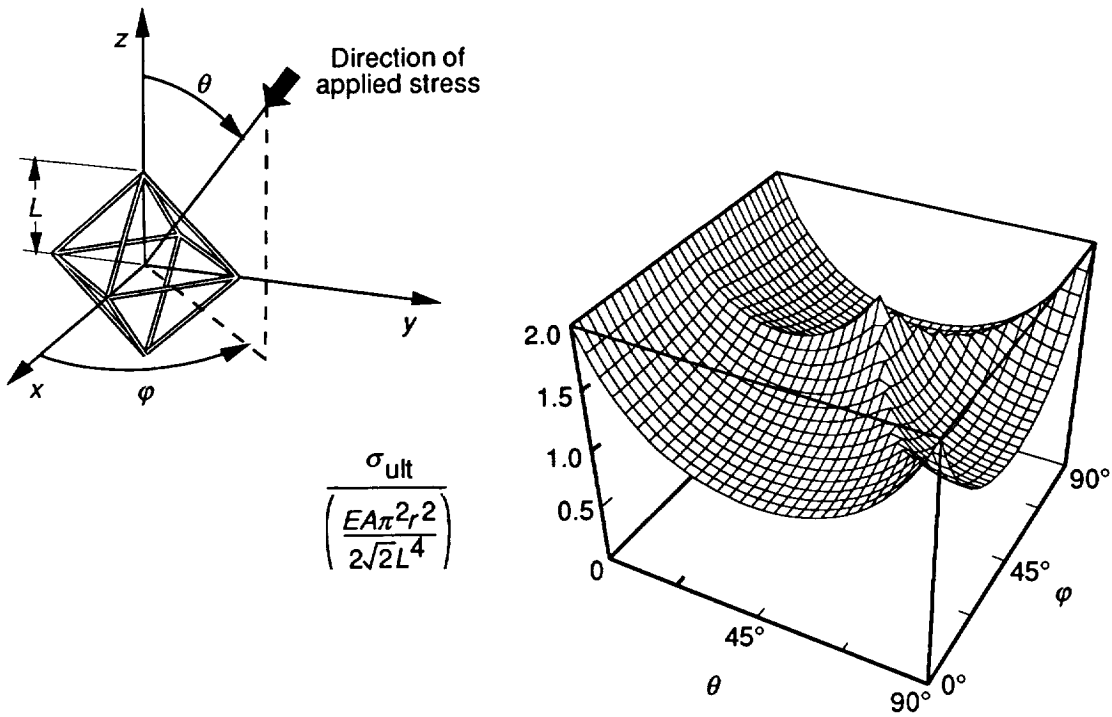
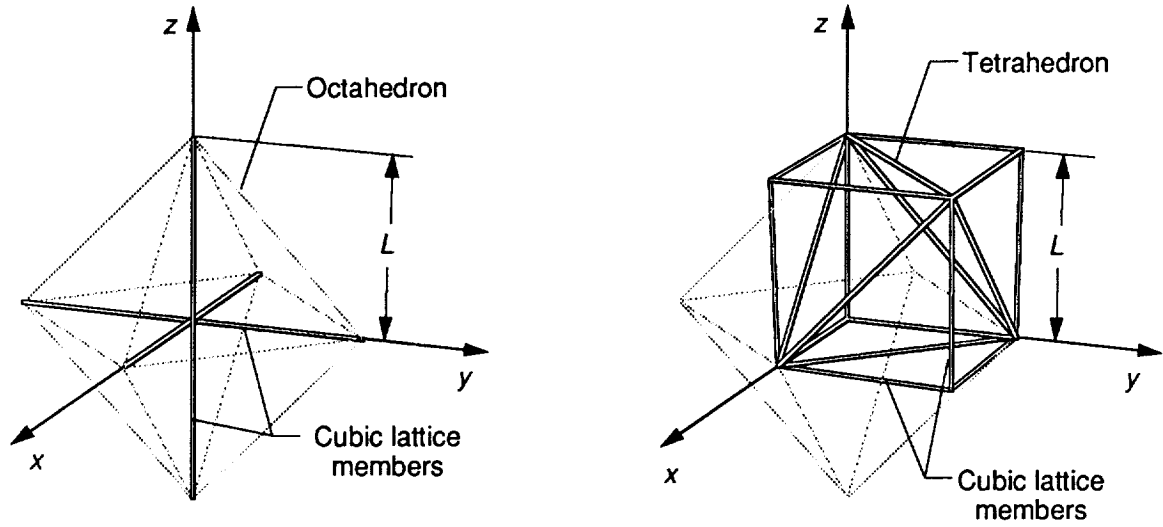


Figure 4. Strength of octahedral truss under uniaxial compression.



(a) Members added to octahedral lattice.

(b) Resulting cubic lattice.

Figure 5. Repeating cell for Warren truss.

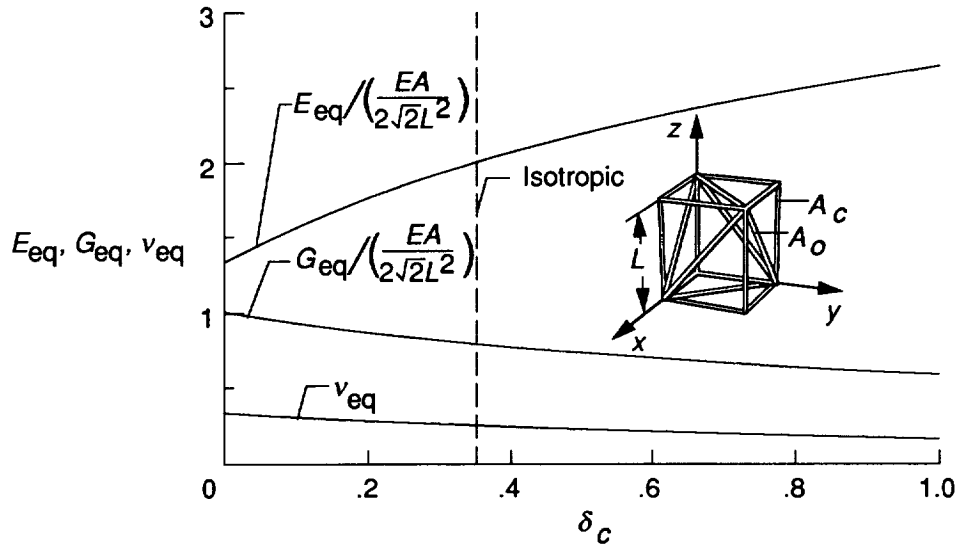


Figure 6. Stiffness tailoring of Warren truss;  $\delta_c = A_c/A_o$ .

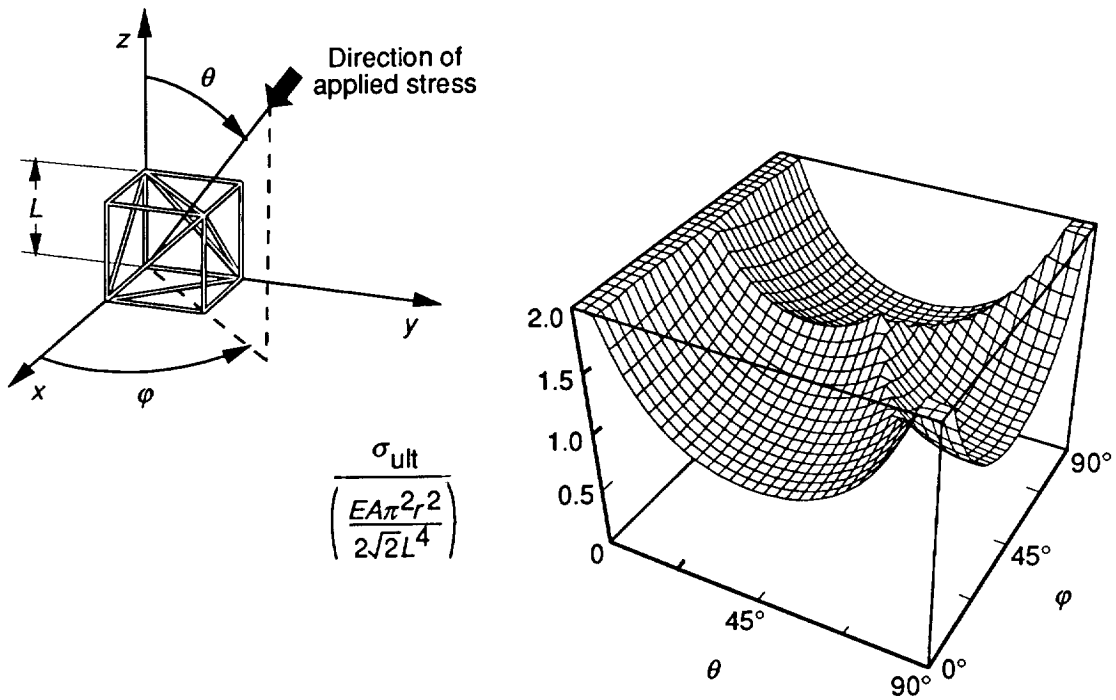


Figure 7. Uniaxial compression strength of isotropic Warren truss. All members have same radius of gyration.

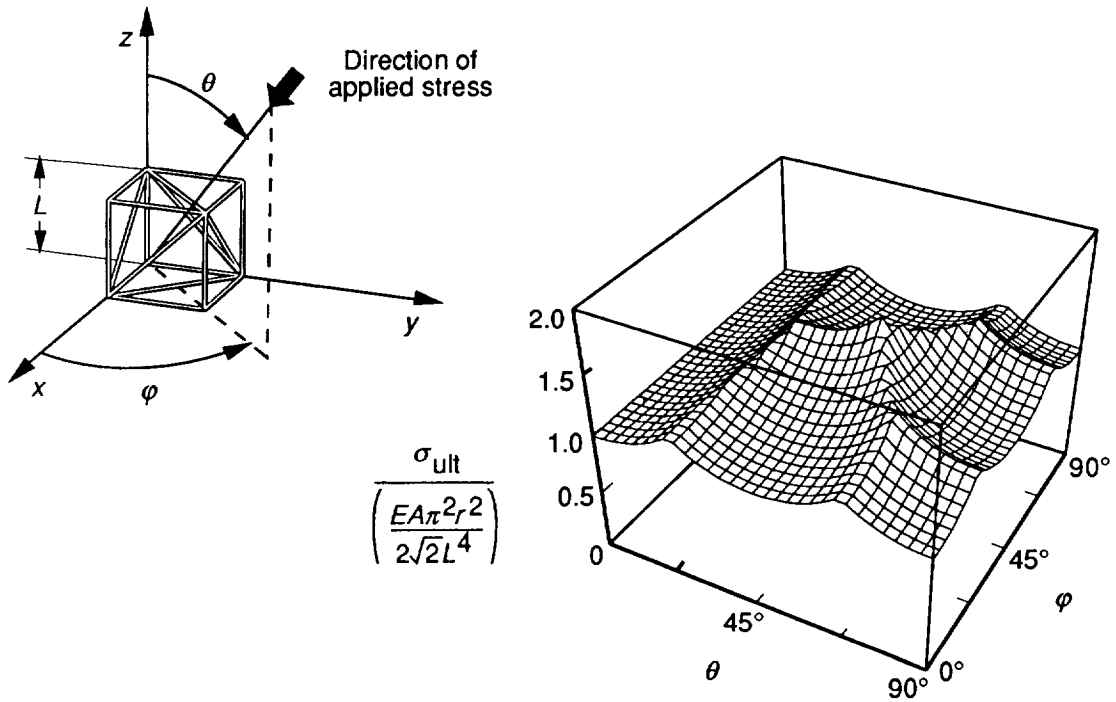


Figure 8. Variation in strength diminished by tailoring all members to have same buckling load.

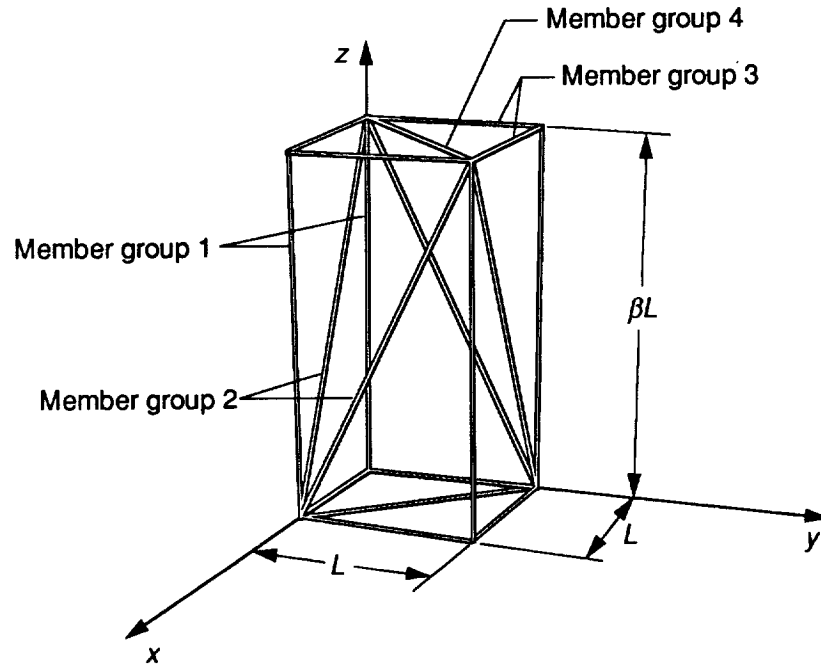


Figure 9. Repeating cell for orthotropic Warren truss.

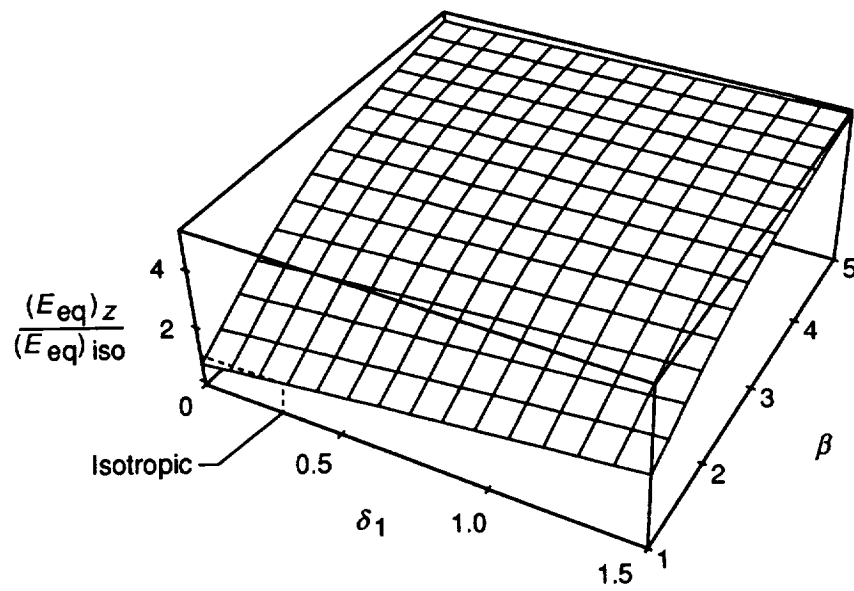


Figure 10. Variation in z-direction Young's modulus with  $\beta$  and  $\delta_1$ .

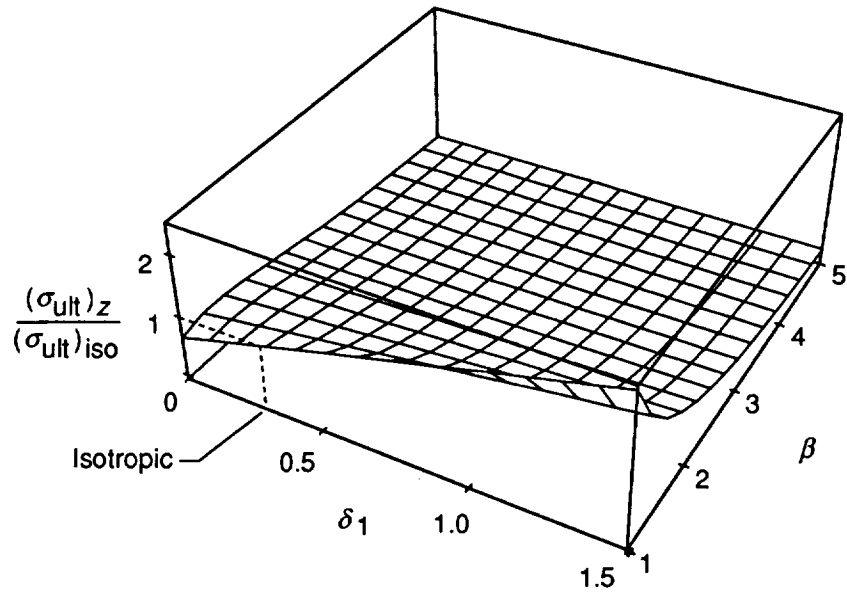


Figure 11. Variation in  $z$ -direction strength with  $\beta$  and  $\delta_1$ .

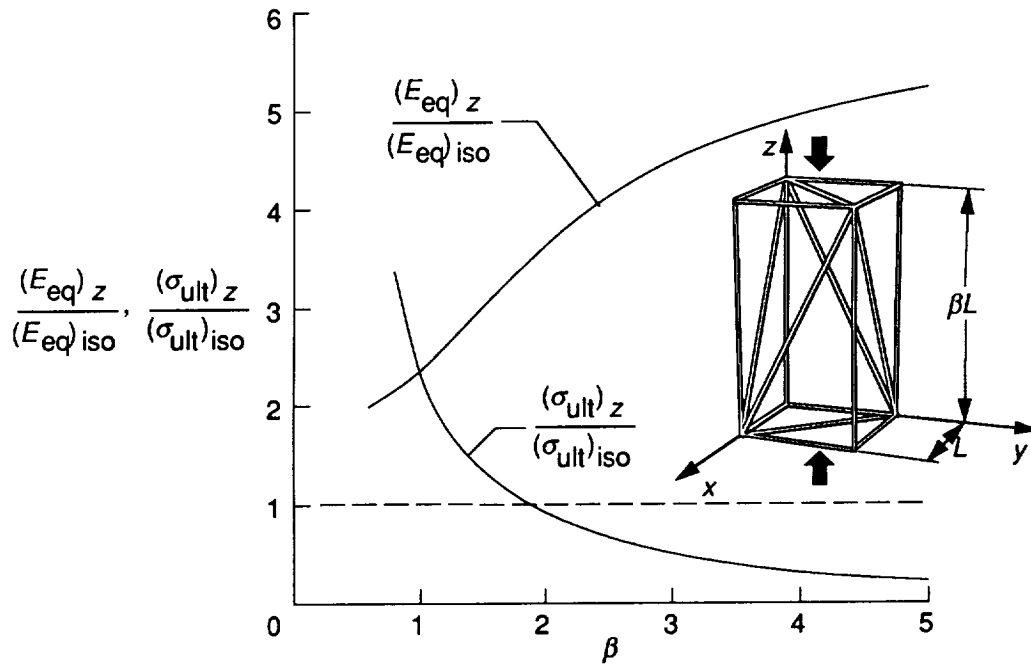


Figure 12. Variation in  $z$ -direction modulus and strength with cell length.

REPORT DOCUMENTATION PAGE			Form Approved OMB No. 0704-0188	
Public reporting burden for this collection of information is estimated to average 1 hour per response, including the time for reviewing instructions, searching existing data sources, gathering and maintaining the data needed, and completing and reviewing the collection of information. Send comments regarding this burden estimate or any other aspect of this collection of information, including suggestions for reducing this burden, to Washington Headquarters Services, Directorate for Information Operations and Reports, 1215 Jefferson Davis Highway, Suite 1204, Arlington, VA 22202-4302, and to the Office of Management and Budget, Paperwork Reduction Project (0704-0188), Washington, DC 20503.				
1. AGENCY USE ONLY (Leave blank)	2. REPORT DATE April 1992	3. REPORT TYPE AND DATES COVERED Technical Paper		
4. TITLE AND SUBTITLE Stiffness and Strength Tailoring in Uniform Space-Filling Truss Structures		5. FUNDING NUMBERS WU 506-43-41-02		
6. AUTHOR(S) Mark S. Lake				
7. PERFORMING ORGANIZATION NAME(S) AND ADDRESS(ES) NASA Langley Research Center Hampton, VA 23665-5225		8. PERFORMING ORGANIZATION REPORT NUMBER L-17001		
9. SPONSORING/MONITORING AGENCY NAME(S) AND ADDRESS(ES) National Aeronautics and Space Administration Washington, DC 20546-0001		10. SPONSORING/MONITORING AGENCY REPORT NUMBER NASA TP-3210		
11. SUPPLEMENTARY NOTES A version of this paper was presented at the Ninth DOD/NASA/FAA Conference on Fibrous Composites in Structural Design, Lake Tahoe, Nevada, November 4-7, 1991.				
12a. DISTRIBUTION/AVAILABILITY STATEMENT Unclassified-Unlimited  Subject Category 39		12b. DISTRIBUTION CODE		
13. ABSTRACT (Maximum 200 words) This paper presents a deterministic procedure for tailoring the continuum stiffness and strength of uniform space-filling truss structures through the appropriate selection of truss geometry and member sizes (i.e., flexural and axial stiffnesses and length). The trusses considered herein are generated by uniform replication of a characteristic truss cell. The repeating cells are categorized by one of a set of possible geometric symmetry groups derived using crystallographic techniques. The elastic symmetry associated with each geometric symmetry group is identified to help select an appropriate truss geometry for a given application. Stiffness and strength tailoring of a given truss geometry is enabled through explicit expressions relating the continuum stiffnesses and failure stresses of the truss to the stiffnesses and failure loads of its members. These expressions are derived using an existing equivalent continuum analysis technique and a newly developed analytical failure theory for trusses. Several examples are presented to illustrate the application of these techniques and to demonstrate the usefulness of the information gained from this analysis.				
14. SUBJECT TERMS Truss; Geometric symmetry; Stiffness tailoring; Strength tailoring; Equivalent continuum analogy; Crystallography		15. NUMBER OF PAGES 28		16. PRICE CODE A03
17. SECURITY CLASSIFICATION OF REPORT Unclassified	18. SECURITY CLASSIFICATION OF THIS PAGE Unclassified	19. SECURITY CLASSIFICATION OF ABSTRACT	20. LIMITATION OF ABSTRACT	